ACS OMEGA

http://pubs.acs.org/journal/acsodf

Article

Enhancing the Oil Recovery from Naturally Fractured Reservoirs Using Viscoelastic Surfactant (VES) Flooding: A Field-Scale Simulation

M. Elmuzafar Ahmed, Amjed M. Hassan, Abdullah S. Sultan,* and Mohamed Mahmoud*

Cite This: *ACS Omega* 2022, 7, 504−517

Read Online

ACCESS | Metrics & More | Article Recommendations

ABSTRACT: A viscoelastic surfactant (VES) has the combined properties of a surfactant and a polymer. Injection of VES fluids into naturally fractured reservoirs (NFRs) can control the mobility of the injected fluid and enhance the total oil recovery. This paper presents a field-scale simulation to evaluate the performance of a noble VES fluid in enhancing the oil recovery from a naturally fractured reservoir. In this work, the results of coreflooding, computerized tomography (CT)-scan, rheology, interfacial tension (IFT), and adsorption measurements were used to build and calibrate a lab-scale model. Thereafter, a chemical enhanced oil recovery (EOR) modeling simulator developed by a computer modeling group (CMG-STARS) was used to build a field-scale simulation. Real seismic data, permeability and porosity distributions, and operating conditions were utilized to develop and evaluate the simulation model. The results show that VES can outperform the surfactant-polymer (SP) flooding and waterflooding in NFRs; VES improved the oil recovery by 10% and reduced the water cut by 47%, at the same conditions. VES reduced the IFT by two orders of magnitude (100 times) compared to waterflooding. Also, VES altered the rock wettability to a more water-wet status, leading to reduce the relative permeability to water (K_{rw}) by a factor of 10, on average. Finally, the simulation study indicated that applying waterflooding after VES flooding leads to a minor increase in the oil recovery. Overall, this study provides a detailed comparison between VES flooding, SP flooding, and conventional waterflooding in NFRs. Sensitivity analysis was performed to study the impact of treatment parameters on the oil recovery from naturally fractured reservoirs. Using actual NFR data, the optimum VES flooding was determined, which will help in conducting VES flooding for real EOR operations.

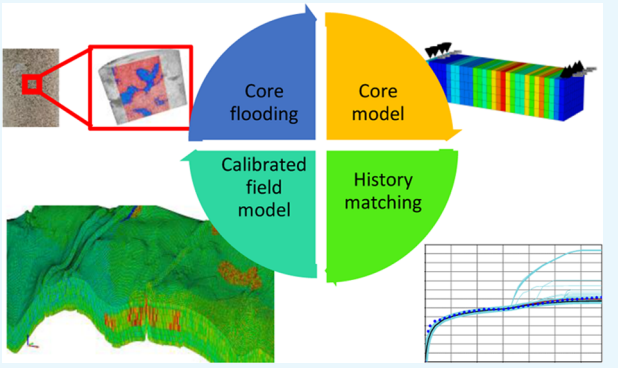

1. INTRODUCTION

Enhanced oil recovery (EOR) methods are applied to increase the oil recovery after primary production.[1] The common EOR techniques are chemical flooding and thermal treatments.[2,3] Different chemicals are injected to improve the flow conditions and enhance the oil recovery. The injected chemicals can affect the rock/oil interface and create favorable flow conditions such as lowering the interfacial tension (IFT), altering the wettability conditions, and improving the oil properties.[1,4] Usually, chemical flooding is implemented after primary production and waterflooding in order to recover the remaining oil.[5] As long as the waterflooding technique is economically feasible, it is preferred. However, waterflooding can increase water production due to the water breakthrough to the production wells.[1,2] Therefore, chemical treatments such as polymer or alkali-surfactant-polymer (ASP) flooding are used to control the fluids' mobility and thereby reduce water production.[6] Nanoparticles can be used with the help of surfactants to improve oil recovery, and nanoparticles are also used to improve the performance of surfactants and delay the water breakthrough.[7] Also, low-salinity brines have been extensively studied in order to improve the efficiency of surfactants and polymers, thereby maximizing the oil recovery.[8] Moreover, after the primary and secondary recovery operations, the remaining oil is trapped in the reservoir pores due to the high capillary and viscous forces.[6,9] Then, chemical treatments are implemented to reduce the capillary and viscous forces. Chemical flooding usually changes the fluids' mobility and reservoir fluid properties, which can create a favorable pressure difference between the reservoir and production wells to recover the remaining oil.[1,4] Although these methods are not capable of recovering the whole remaining oil saturation in the reservoir, a substantial amount of oil can be recovered from the reservoir.[4,10−12]

Received: September 6, 2021
Accepted: November 15, 2021
Published: December 28, 2021

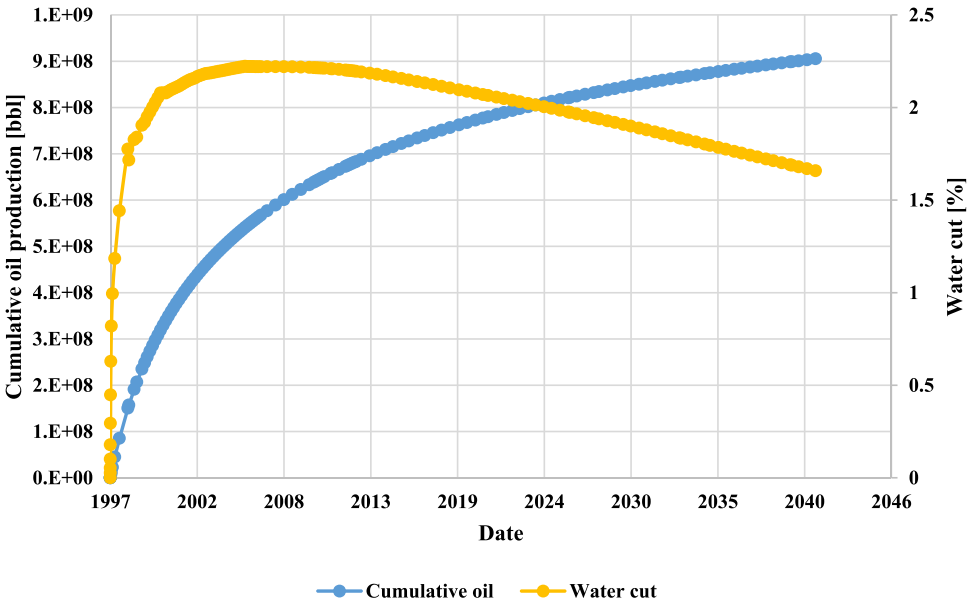

Figure 1. Natural field production for 45 years, cumulative oil production, and water cut.

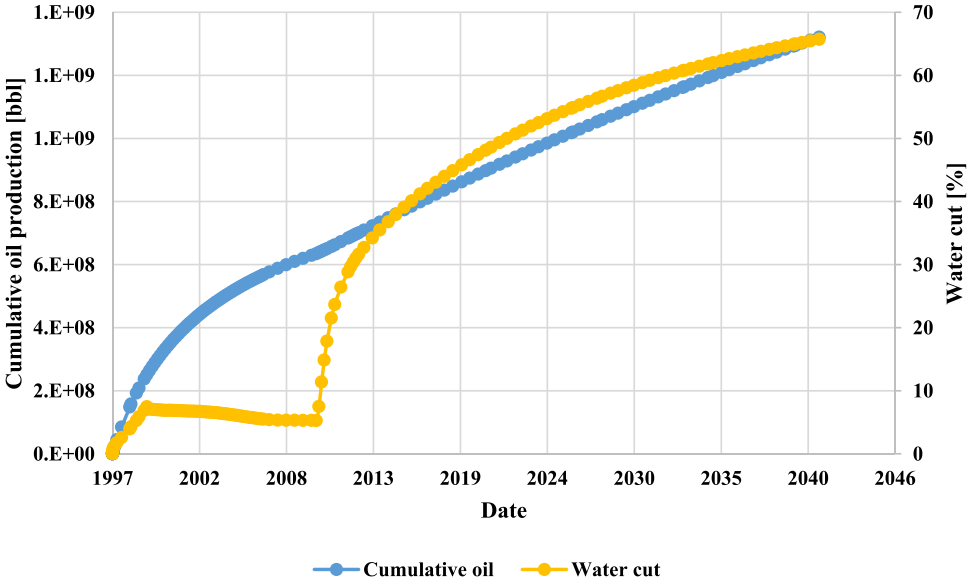

Figure 2. Natural field production for 13 years, then waterflooding for 31 years, cumulative oil production, and water cut.

In recent years, viscoelastic surfactant (VES) flooding has gained much importance because of its dual capability to mobilize the trapped oil.[13−15] Both the mobility ratio and capillary number are affected using VES as an EOR fluid. It provides better displacement of the trapped fluid and recovers the remaining oil by reducing the IFT; thus, it has the qualities of both surfactants as well as polymers.[10,16−18] In general, viscoelastic fluids are non-Newtonian fluids and they combine both elastic and viscous properties.[19] During VES flooding, the injected fluids mobilize the remaining oil by improving the mobility ratio and reducing the IFT. Consequently, VES flooding can increase the displacement efficiency and oil recovery significantly.[20−22] In addition, the stability of the injected chemicals is a major issue while employing them in EOR operations. The major issue with using polymer flooding and surfactant flooding is that most of the polymers degrade at high temperatures, and the surfactant tends to precipitate upon exposure to divalent cations and will partition to the oil phase at high salinities. In such situations, viscoelastic surfactant flooding presents an effective option because it has the chemical formulations of both a polymer and a surfactant.[23] A viscoelastic surfactant has excellent thermal stability and resistivity to salinity, and thereby VES flooding can significantly enhance the oil recovery from both sandstone and carbonate reservoirs.[11,14,16−18]

Most of the research studies conducted for VES were for fracturing applications[24,25] while very limited studies were for EOR.[26] However, limited simulation studies were performed to assess the effectiveness of VES treatment on a large scale, especially for naturally fractured reservoirs (NFRs). Also, most of the available studies utilize some of the VES mechanisms, without combining all effective VES characteristics that contribute to the oil recovery. The novelty of this work is in incorporating the different recovery mechanisms during the VES flooding, using actual reservoir data. This study aims to evaluate the performance of a noble VES in enhancing the oil recovery

https://doi.org/10.1021/acsomega.1c04900
ACS Omega 2022, 7, 504−517

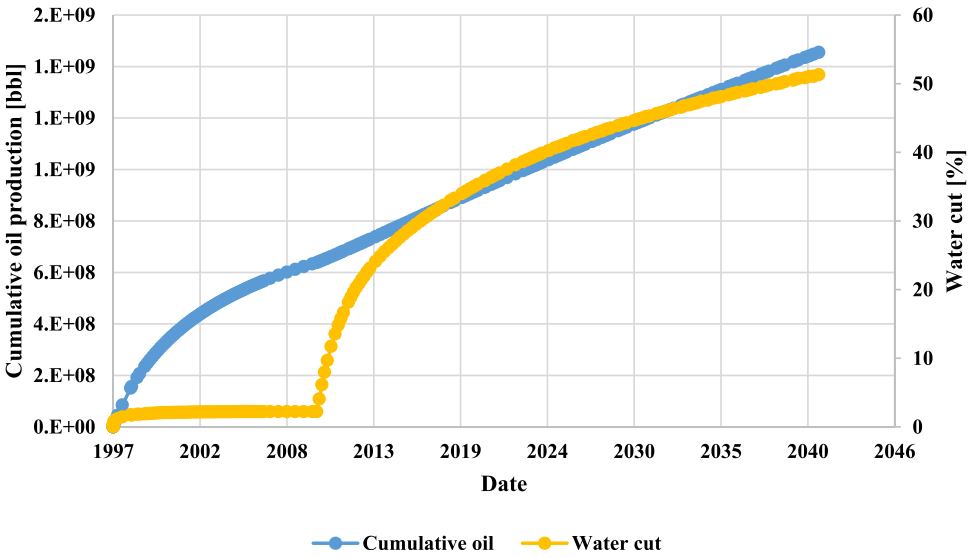

Figure 3. Natural field production for 13 years, then chemical flooding for 31 years, cumulative oil production, and water cut.

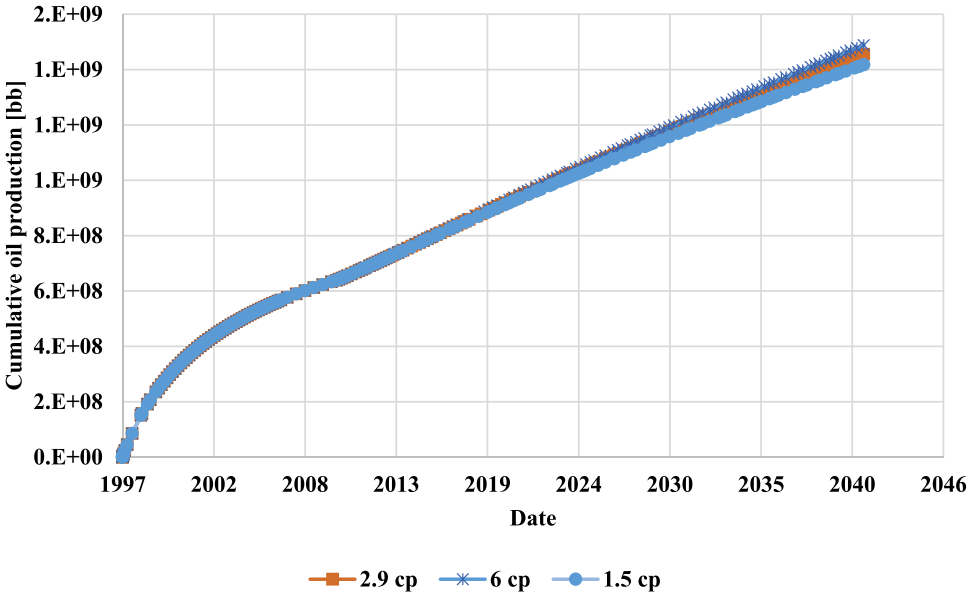

Figure 4. Cumulative oil production profiles for different VES viscosities.

from NFR using field-scale simulation. A detailed comparison between waterflooding and VES flooding is presented. Also, a sensitivity analysis for different operation parameters is conducted to suggest the optimum flooding conditions that can maximize the oil recovery. First, a lab-scale simulation was carried out utilizing experimental measurements such as coreflooding, computerized tomography (CT)-scan, rheology, IFT, and adsorption experiments. Then, model calibration and history matching were performed to improve the reliability of the simulation model. Thereafter, a field-scale simulation was carried out using actual reservoir conditions, and different treatment conditions were examined. The profiles of oil production, water cut, and reservoir pressure were thoroughly analyzed.

2. RESULTS AND DISCUSSION

Middle East reservoirs are usually characterized as high-temperature and high saline (HTHS) reservoirs. It is reported that less than 20% of the chemical EOR projects were conducted in carbonate reservoirs, especially in the Middle East, where few small-scale pilots were tested.[27] Also, Middle East carbonates are highly heterogeneous and have complex pore characteristics with wettability variation from mixed to oil-wet status. The reservoir conditions within this region can be summarized as HTHS conditions. Carbonate reservoirs are usually characterized as a low permeability matrix with fractures, while a considerable portion present a high permeability matrix with fractures,[28] which may reduce the efficiency of conventional chemical flooding treatments. The VES technique presents an effective technique in such conditions that can enhance oil recovery and reduce water production. In this work, three different scenarios were examined to evaluate the performance of VES treatment. Natural production, seawater (SW) flooding, and VES flooding scenarios were simulated. The injection of seawater and VES was started after 13 years of natural production. A long-term production strategy was applied to assess the reliability of the simulated models; the ultimate oil recovery was estimated for 45 years of production.

https://doi.org/10.1021/acsomega.1c04900
ACS Omega 2022, 7, 504−517

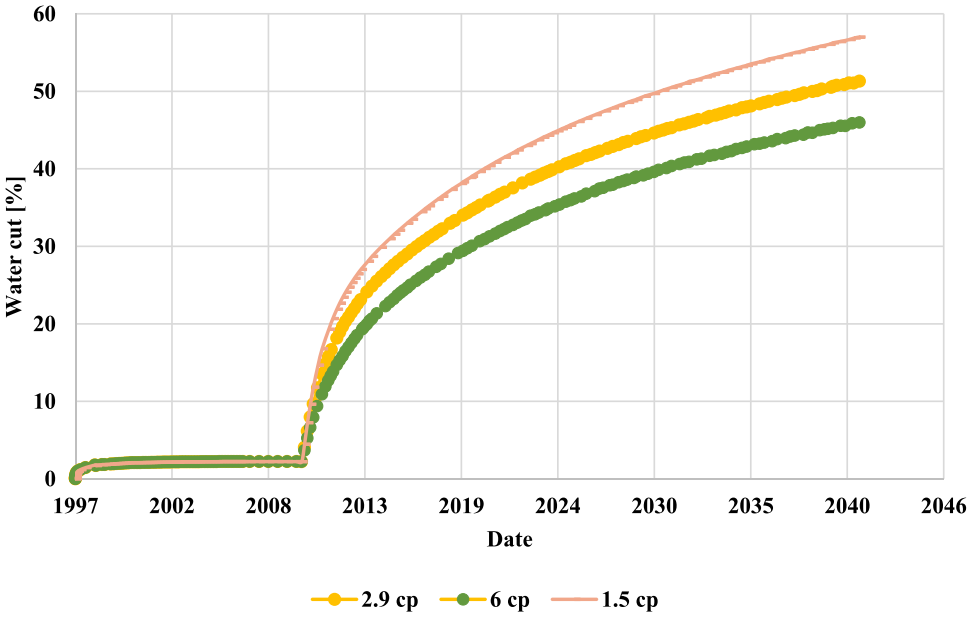

Figure 5. Water-cut profiles for different VES viscosities: increasing the viscosity of the injected fluid led to a decrease in the water cut.

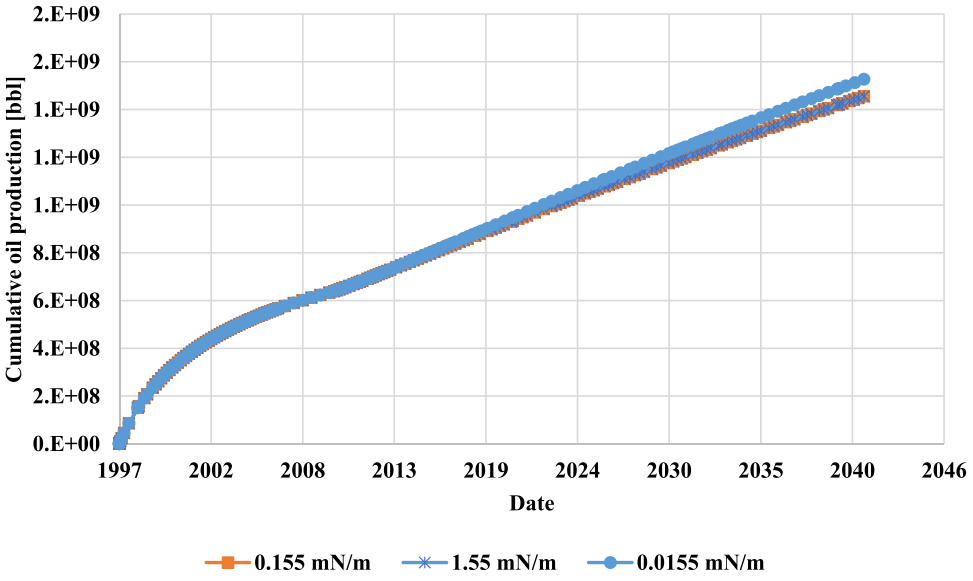

Figure 6. Cumulative oil production profiles for different IFT values; decreasing the IFT led to an increase in the oil production.

2.1. Natural (Primary) Production. Figure 1 shows the plot of water-cut and cumulative oil production during the 45 years' natural production period. The water cut increased up to a maximum value of 2.25%, then decreased gradually to a value of 1.6% at the end of the production period. This low water-cut value is attributed to the excellent well placement in the oil zone in this volumetric reservoir with no water drive. The cumulative oil production was increasing rapidly in the first five years as the well started with a high production rate due to the high initial reservoir pressure. However, the reservoir is soon depleted due to the lack of pressure support and the increment curve is slightly flattened. The cumulative production at the end of the period is 905.2 million STB.

2.2. Waterflooding Treatment. Figure 2 depicts the change of water-cut and cumulative oil production during the 13 years' natural production followed by 31 years of waterflooding to maintain the reservoir pressure and enhance the sweep efficiency. In the first period, the water cut was very low because there was no water influx and the production wells were placed in the oil zone; thereafter, the water cut started to increase gradually when the waterflooding started. The water cut reached a high value of 66% at the end of the waterflooding period. On the other hand, the cumulative oil production started to increase rapidly when the reservoir pressure was strong, then turned to a flatter slope at a later time of natural production. The slope became steeper again with the introduction of waterflooding due to pressure increase. At the end of natural production, 634.66 million STB were recovered, which then increased to 1321.2 million STB by the end of waterflooding.

2.3. VES Flooding Treatment. The water-cut and cumulative oil production for VES flooding following a period of natural production are shown in Figure 3. The water cut followed the same trend as in the waterflooding due to the same reason; however, the water mobility is lower in this case due to

https://doi.org/10.1021/acsomega.1c04900
ACS Omega 2022, 7, 504−517

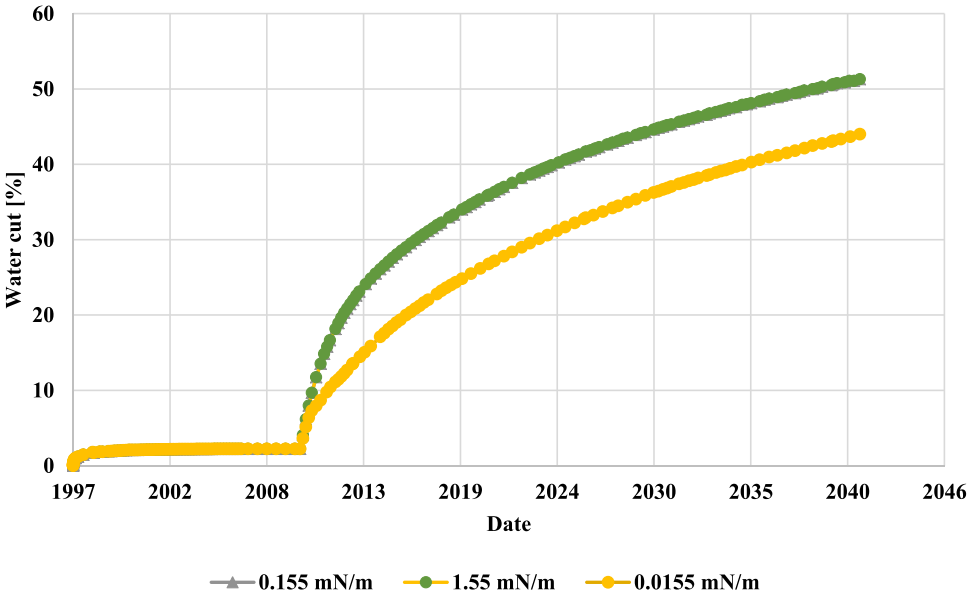

Figure 7. Water-cut profiles for different IFT values; decreasing the IFT led to reducing the water cut.

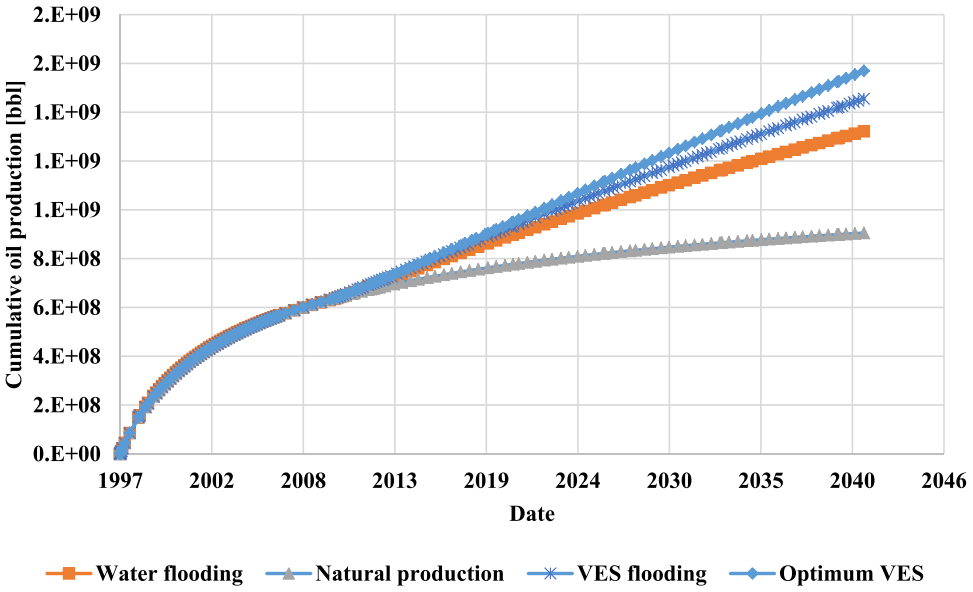

Figure 8. Comparing different scenarios for VES flooding, utilizing the cumulative oil production.

the introduction of the viscous VES solution. The final water cut is only 51% compared to the one in the waterflooding, which was 66%. The same waterflooding trend was noticed in the VES flooding, but the final oil produced is higher in VES flooding (1455.096 million STB compared to 1321.2 million STB from waterflooding).

2.4. Viscosity Sensitivity. This set is made to investigate the effect of viscosity on the water-cut and cumulative oil production in the VES flooding. Three different viscosities were investigated: 1.5, 2.9, and 6 cp. Figure 4 shows the cumulative oil recovery and Figure 5 shows the water cut. The results confirm our theory: the higher the viscosity, the better the sweep efficiency and hence the recovery. The same goes for the water cut: the higher the viscosity, the lower the water mobility and hence the lesser the water cut.

2.5. IFT Sensitivity. Another set was conducted to study the effect of IFT on the cumulative oil production and the water cut, as shown in Figures 6 and 7, respectively. No difference was noticed in the cumulative oil production at 0.155 and 1.55 mN/m, but at 0.0155 mN/m, a higher oil production was observed. This could be attributed to the concept of critical capillary number for de-trapping, at which the trapped oil starts moving; hence, 1.55 and 0.155 mN/m are not enough to mobilize the trapped oil, while 0.0155 can mobilize a considerable volume of the trapped oil. The water cut for the 0.155 and 1.55 mN/m remained the same because no more oil was mobilized when a lower IFT value was used. However, reducing the IFT can lead to increasing the capillary number above the critical limit and hence mobilize the oil and increase the ultimate recovery.

2.6. Comparison. The optimum conditions for VES flooding were determined based on the sensitivity analysis of IFT and viscosity. Applying the optimum VES injection showed a considerable increase in the VES performance. Figure 8 shows the profiles of cumulative oil production for natural production,

https://doi.org/10.1021/acsomega.1c04900
ACS Omega 2022, 7, 504−517

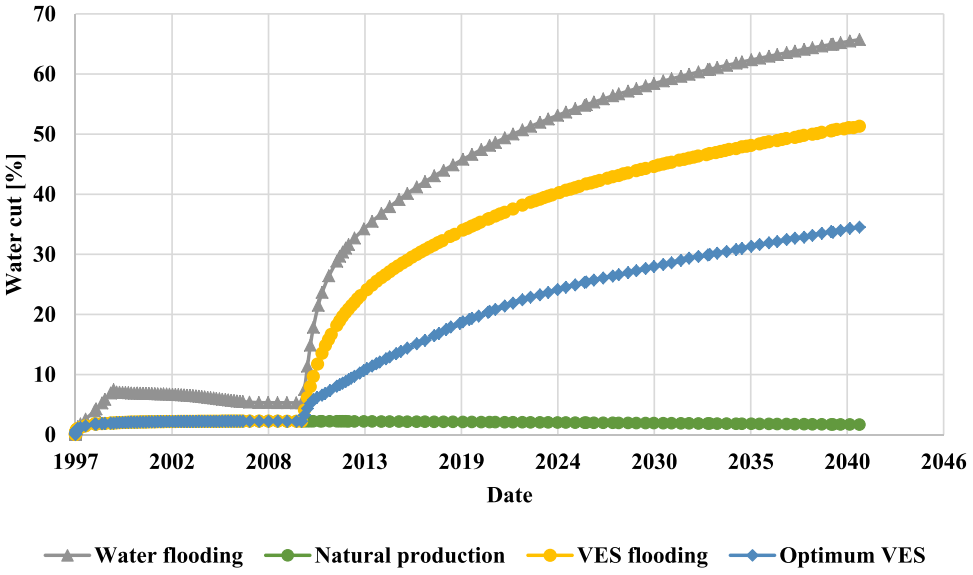

Figure 9. Comparing different scenarios of VES flooding; results for water-cut profiles.

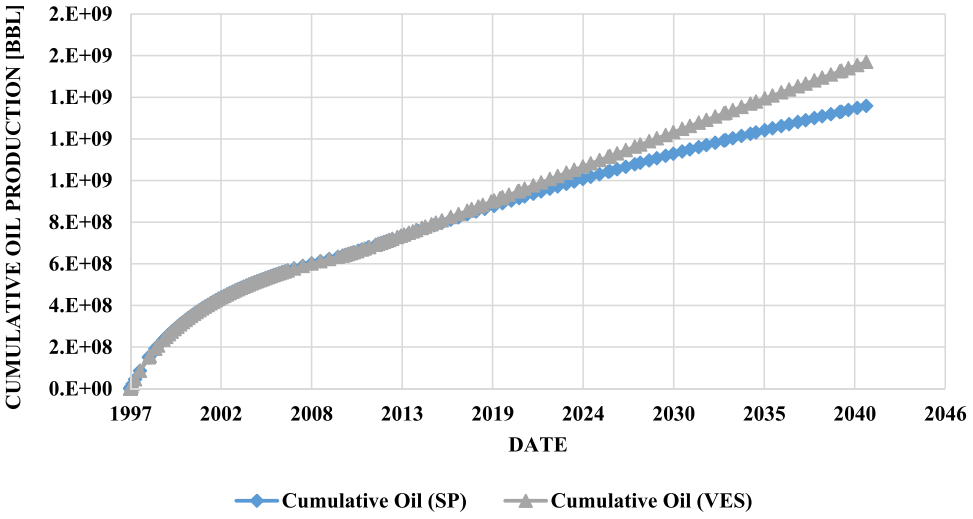

Figure 10. Comparing VES flooding with SP flooding; results for cumulative oil production.

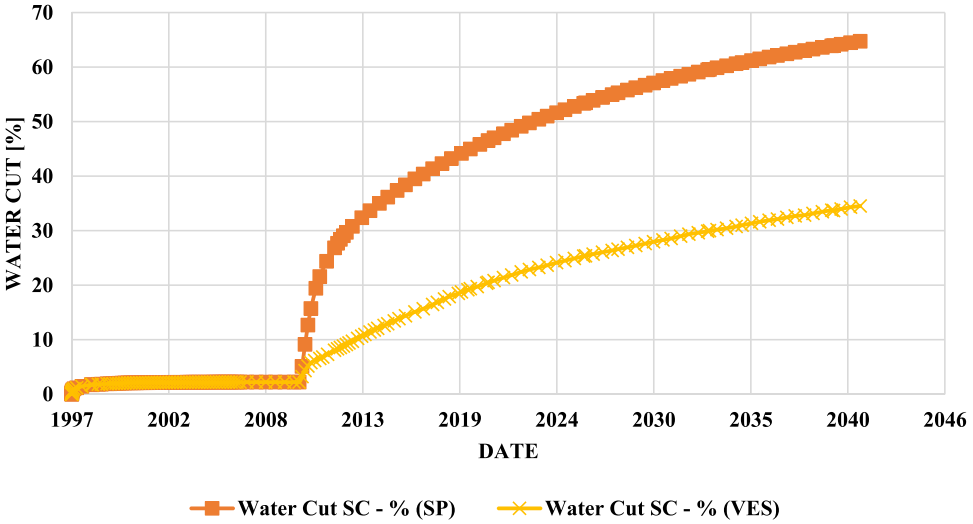

Figure 11. Comparing VES flooding with SP flooding; results for water-cut profiles.

https://doi.org/10.1021/acsomega.1c04900
ACS Omega 2022, 7, 504−517

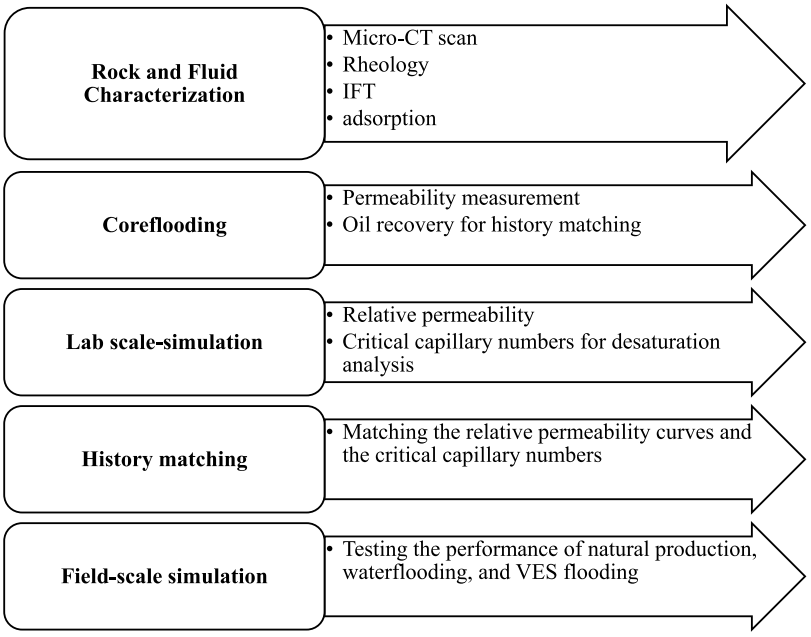

Figure 12. Summary of the methodology followed in this study.

waterflooding, base case of VES flooding, and optimum VES flooding. The cumulative recovery from waterflooding is 46% higher than that of natural production, and the base-case VES flooding increased the oil recovery by 60.7% higher compared to the natural production, while the optimum VES flooding increased the oil production by 73.3% compared to the primary oil production. Moreover, the impact of injecting water again after VES flooding was examined, and a minor increase in the oil recovery was achieved (less than 1%). The plot of water cut is shown in Figure 9: the natural production has the lowest water-cut value due to the good well placement and perforation in the oil zone with the volumetric reservoir with no water drive. The traditional waterflooding showed the highest water-cut value of 65.7%, while the base case of VES flooding provided a 22% less water cut compared to waterflooding. The optimum case of VES flooding reduced the water cut by 47.8% compared to traditional waterflooding.

Another comparison was carried out between the VES flooding and SP flooding, which in principle have the same recovery mechanisms in terms of mobility control and IFT reduction. SP performance was tested in coreflooding using successful chemical candidates through a long screening process in terms of stability, rheology, IFT, and phase behavior.[29] The polymer used was acrylamide tertiary butyl sulfonate (ATBS)/acrylamide (AM) copolymer and the surfactant was amphoteric carboxybetaine, with their optimum concentrations in the simulation to compare it with the VES. The VES achieved a 15.5% higher recovery than the SP flooding as shown in Figure 10, while the VES has a 30% less water cut than SP as shown in Figure 11.

3. CONCLUSIONS

This paper presents a field-scale simulation to evaluate the performance of a noble viscoelastic surfactant (VES) fluid in enhancing the oil recovery from naturally fractured reservoirs (NFR). Real seismic data and actual reservoir conditions were used to develop the simulation model, and history matching was performed to calibrate the developed model. Sensitivity analysis was conducted to determine the optimum flooding conditions that maximize the oil recovery and reduce the water cut. Based on this study, the following conclusions were achieved:

- Viscoelastic surfactant flooding outperforms conventional waterflooding; VES improved the oil recovery by 10% and reduced the water cut by 47% compared to waterflooding, at the same conditions.
- The increase in oil recovery during VES flooding is attributed to the IFT reduction, wettability alteration, and mobility control mechanisms. VES reduced the IFT by two orders of magnitude (100 times) and reduced the relative permeability to water (K_{rw}) by a factor of 10 compared to waterflooding.
- The simulation study indicates that applying waterflooding after VES flooding leads to a minor increase in the oil recovery.
- Overall, this study will help in conducting VES flooding for real EOR operations by providing the optimum conditions for VES flooding.

4. MATERIALS AND METHODOLOGY

The methodology followed in this study is described in Figure 12. Generally, the work was conducted in three stages: material characterization (rock and fluid analysis), coreflooding, and simulation study. At the first stage, micro-CT scan and rheology

Table 1. Formation and Seawater Brine Compositions Used for Rock Saturation and Flooding Experiments

ions	MW	FW ppm	SW ppm
Na^+	23	66 160.90	18 509.35
Ca^{++}	40	18 985.16	649.15
Mg^{++}	24.8	2279.60	2148.24
HCO_3^-	61.0168	384.18	119.83
Cl^-	35.45	140 572.15	32 183.57
SO_4^-	80.06	1521.05	4028.40
TDS		229 903.05	57 638.54

https://doi.org/10.1021/acsomega.1c04900
ACS Omega 2022, 7, 504−517

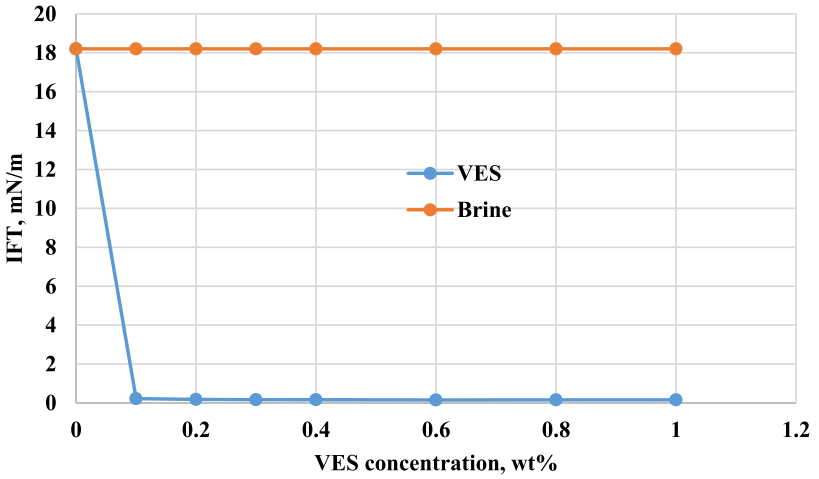

Figure 13. IFT for VES and brine; IFT was reduced by 110 times (two order of magnitude) using VES compared to brine, at ambient pressure and 80 °C.

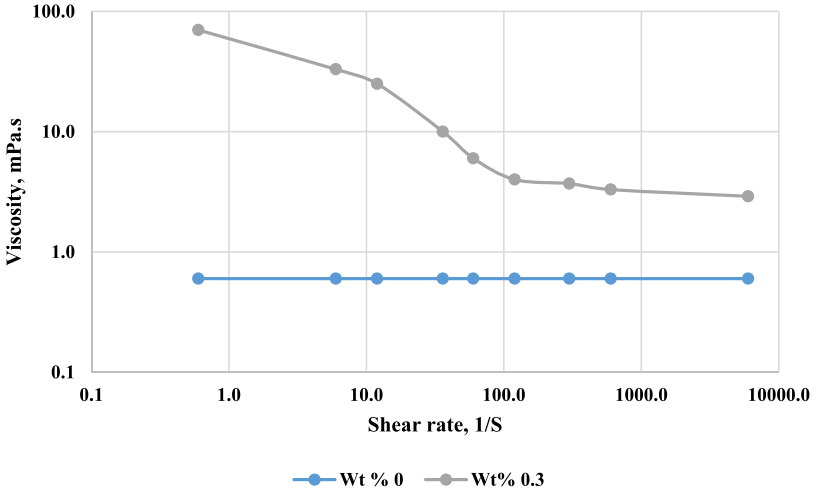

Figure 14. Viscosity against shear rates for brine and optimum VES concentration, at ambient pressure and 80 °C.

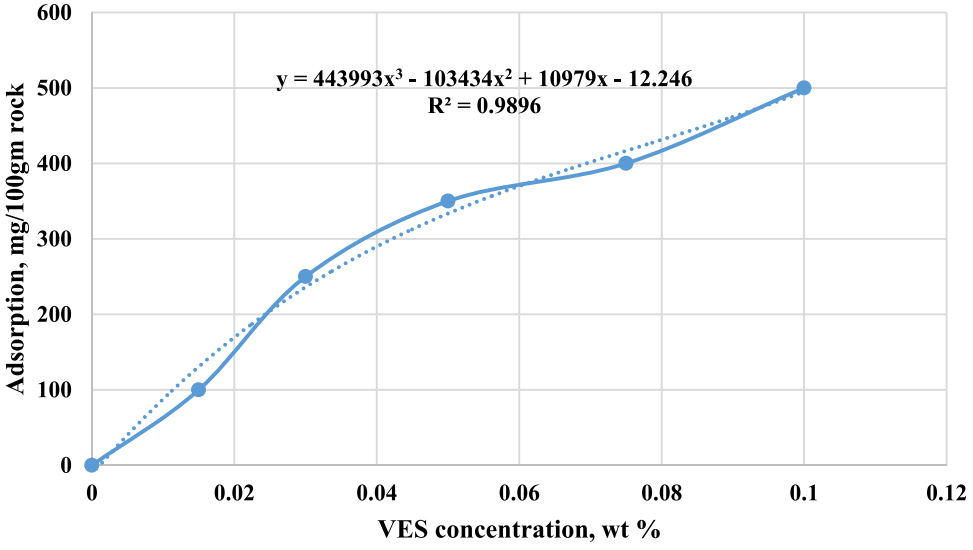

Figure 15. VES adsorption against concentration; a polynomial model was observed for the carbonate sample at 60 °C.

measurements were conducted, as well as an adsorption study. Thereafter, coreflooding experiments were carried out to assess the oil recovery using the chemical injection. Finally, a detailed simulation study was performed utilizing the results of laboratory measurements, and history matching was used to validate and calibrate the simulation model.

https://doi.org/10.1021/acsomega.1c04900
ACS Omega 2022, 7, 504−517

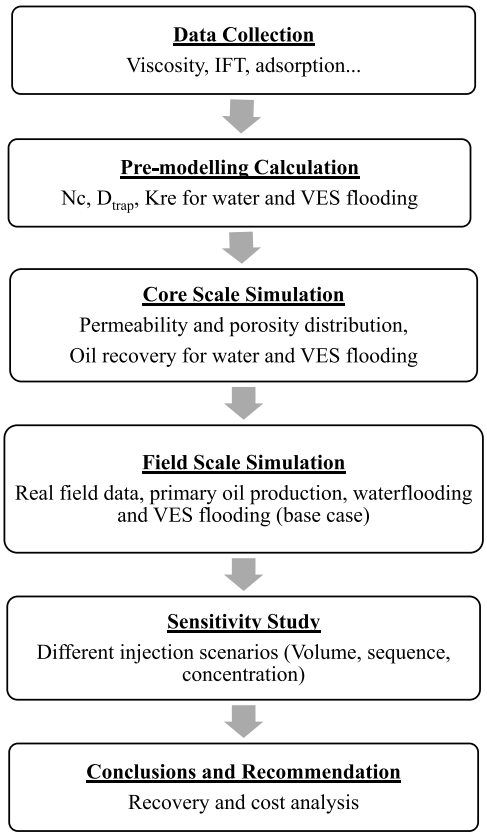

Figure 16. Workflow for the simulation study.

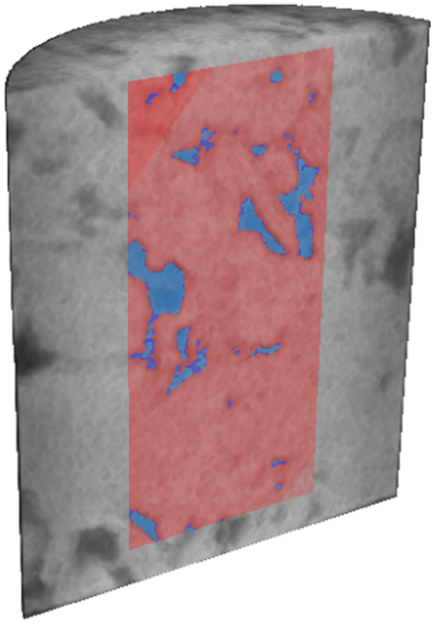

Figure 17. Micro-CT image of a core sample; the porosity and permeability distributions were generated utilizing the micro-CT results.

4.1. Materials. *4.1.1. Brine.* Two different synthetics brines were used: formation water brine (FW) with total dissolved solids (TDS) of 229 903 ppm, and seawater (SW) with TDS of 57,638 ppm. Table 1 shows the ionic composition of the brines that were used for rock saturation and during the waterflooding experiments, as well as for preparing the chemical solution.

4.1.2. Surfactant. The surfactant used in this work is Armovis EHS viscoelastic surfactant (VES), which is an amphoteric surfactant produced by Nouryon company. Different VES concentrations were examined to find the best chemical concentration that can provide better IFT values. Among all tested concentrations, 0.3 wt % was selected as the optimum one, which provides the required IFT above the critical micelle concentration (CMC) as shown in Figure 13. The VES viscosity was investigated as a function of the shear rate for the 0.3 wt % concentration as shown in Figure 14. Also, the VES adsorption was studied, and the results are provided in Figure 15. It should be noted that the simulation model was developed utilizing the IFT, viscosity, and adsorption results.

4.1.3. Crude Oil. Heavy crude oil was used in the coreflooding experiments, and its properties were used in the simulation model. The used oil has a viscosity of 10 cP at 90 °C and an API gravity of 17. Also, it contains 37% saturates, 46% aromatics, 7% resins, and 10% asphaltene according to the SARA analysis.

4.2. Methodology. The work methodology is presented in Figure 16: first, the experimental data were collected, then, pre-modeling calculations were conducted to determine the capillary numbers (N_c) and relative permeability curves. Thereafter, a core-scale simulation was conducted based on real permeability and porosity distributions, and the oil recovery from the rock sample was validated utilizing the coreflooding experiment. The core-scale model was calibrated, and history matching was performed to improve the accuracy of the simulation model. After this, a field-scale simulation was carried out using a real reservoir seismic, and the performance of primary production, waterflooding, and VES flooding was studied. Finally, a sensitivity analysis was conducted to examine the impact of several parameters on the oil recovery, and the optimum scenario is suggested.

4.2.1. Rock Model from Micro-CT. Micro-CT scanning was performed using an Xradia (new Zeiss) Versa XRM-500 device, which is a three-dimensional (3D) X-ray microscopy equipment used for non-destructive tomography. Indiana limestone rocks were imaged, and the CT-scan images were used to develop the lab-scale model. The micro-CT images were analyzed using PerGeos software to produce high-quality porosity distribution for the scanned portion of the core samples (as shown in Figure 17). Then, a full-porosity distribution was determined for the whole rock sample, assuming the same portion distribution as the small portion. The final distribution is provided in Figure 18. Thereafter, the permeability map was generated based on the porosity distribution. Based on the permeability and porosity measurements, the permeability−porosity relationship can be described using eq 1. Figure 19 shows the permeability distribution for the studied rock samples.

$$K = 264*\varnothing \quad (1)$$

where K is the absolute rock permeability in mD and $\varnothing$ is the total rock porosity in fraction.

4.2.2. Relative Permeability. The basic concept of modeling different chemical injections is mainly controlled by the capillary numbers and relative permeability. Injection of chemical fluids (such as VES) after waterflooding can lead to a change in the capillary numbers and hence the relative permeability curves will be changed, resulting in mobilizing the trapped oil and hindering the fast-moving water by introducing viscosity control. In this work, two different interpolation sets of relative permeability curves were used to address this behavior. The first set represents the waterflooding condition, and the second set

https://doi.org/10.1021/acsomega.1c04900
ACS Omega 2022, 7, 504−517

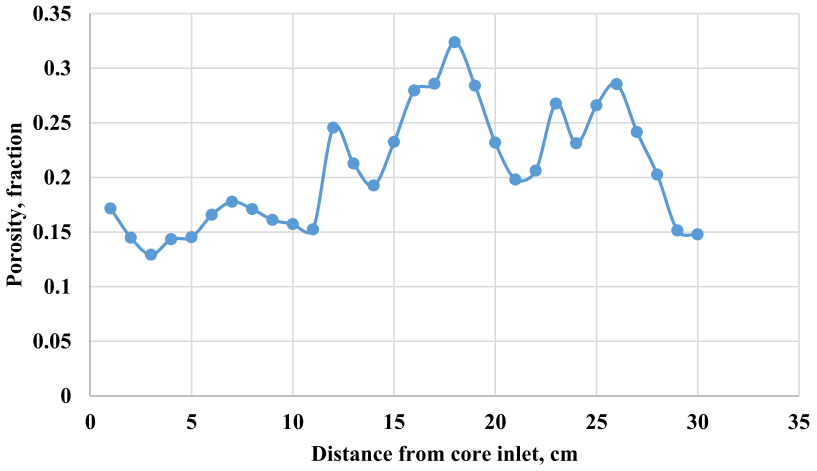

Figure 18. Porosity distribution for the used rock sample.

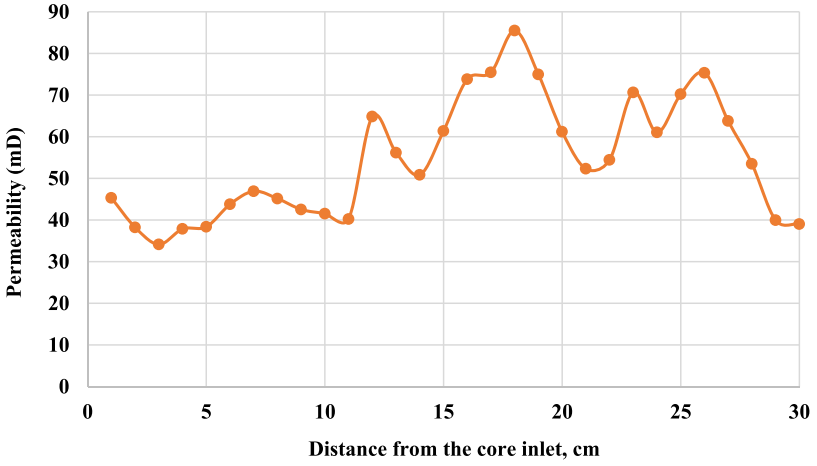

Figure 19. Permeability distribution for the used rock sample.

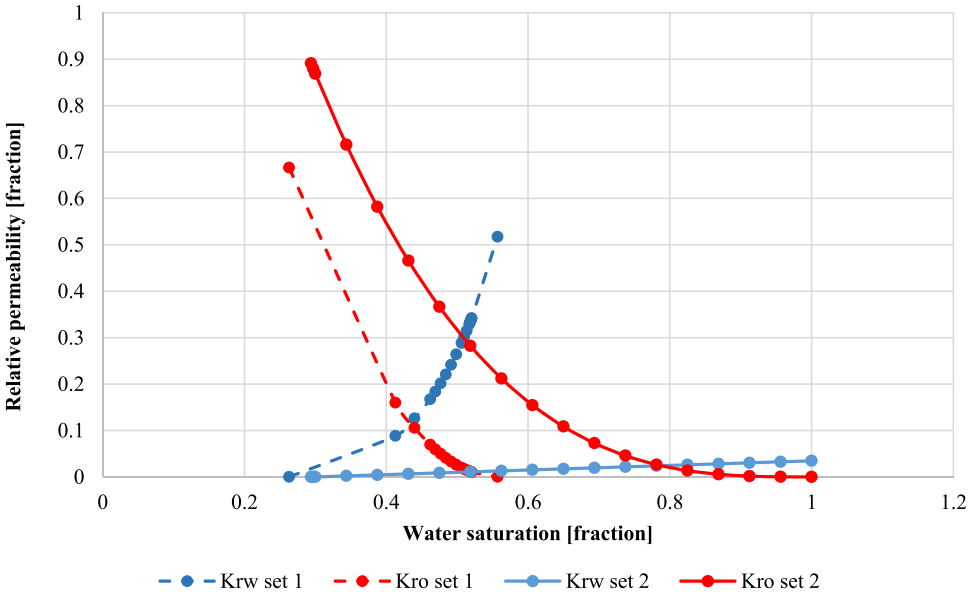

Figure 20. Relative permeability curves for waterflooding (set 1) and VES flooding (set 2) using VES lead to reduce the relative permeability to water by more than 90%.

represents the chemical flooding situation. The capillary number was used to shift from one set to another based on the duration of each flooding phase. The results of coreflooding experiments were utilized to determine the relative permeability curves.

https://doi.org/10.1021/acsomega.1c04900
ACS Omega 2022, 7, 504−517

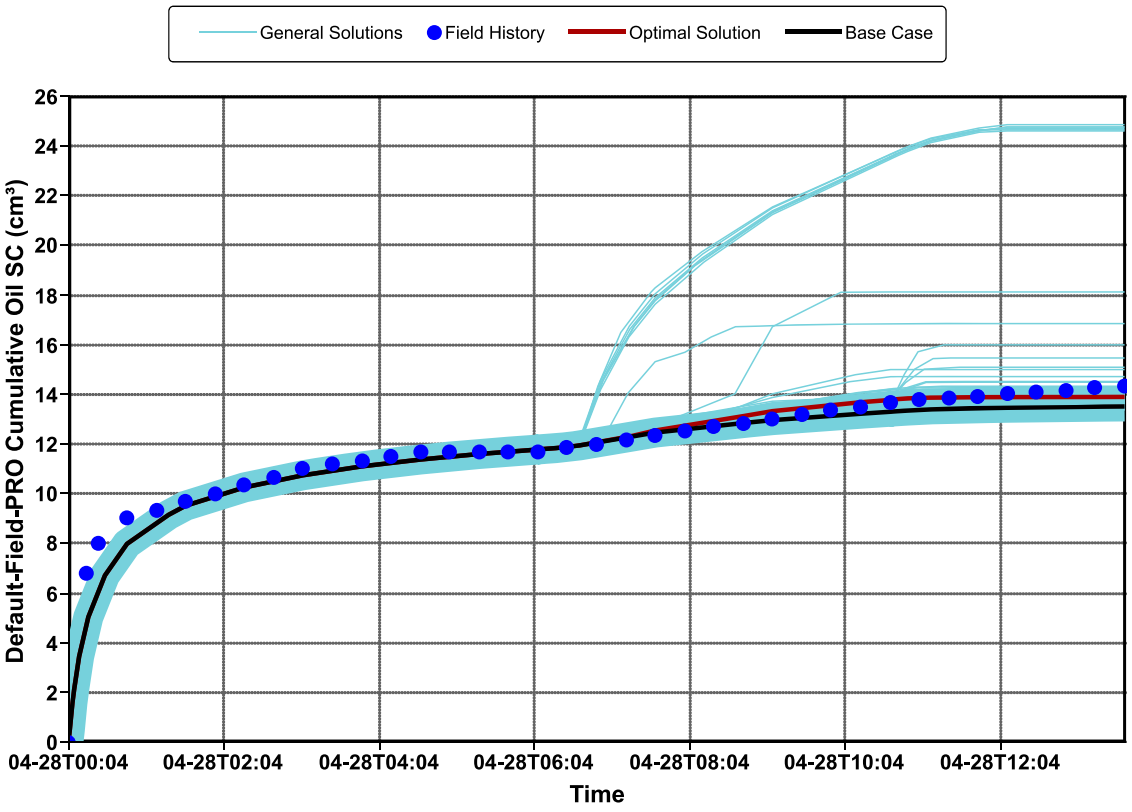

Figure 21. Results of history matching for the cumulative oil production, till getting the optimum match between the experimental results and model outputs for water and VES floodings.

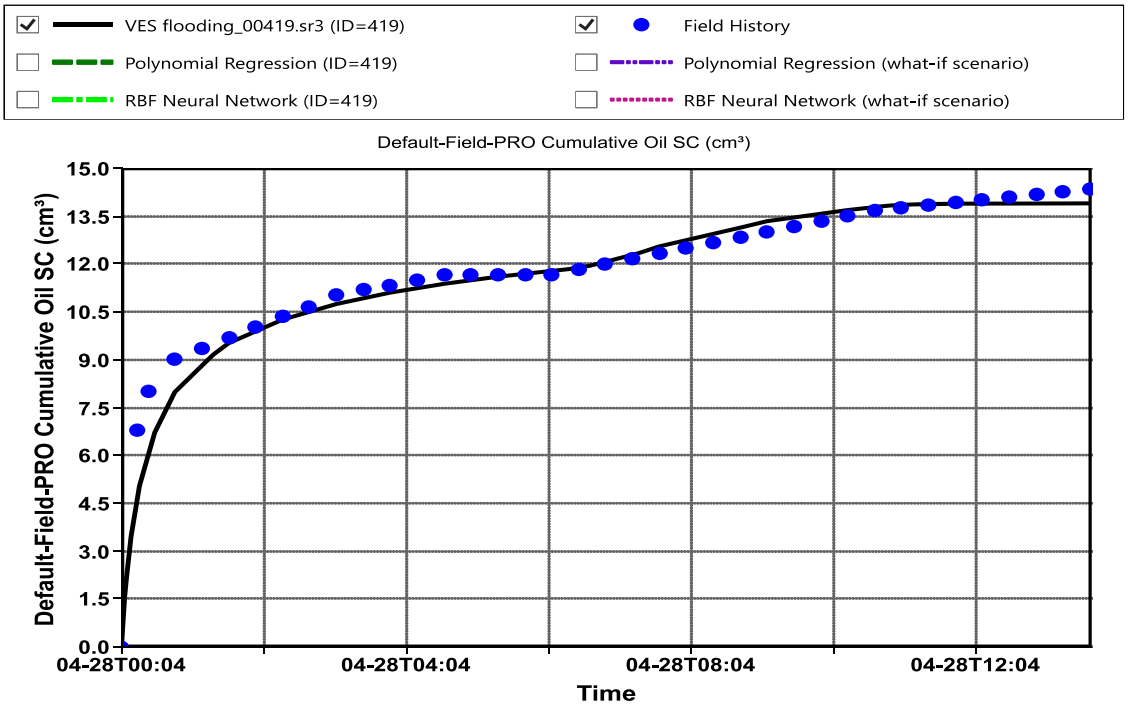

Figure 22. Optimal match for the cumulative oil production obtained from the coreflooding experiment and simulation model.

Endpoint saturations were used to estimate the relative permeability values at the end of waterflooding. However, a full oil mobilization approach was assumed during the chemical injection, and the relative permeability curves were calculated accordingly. Figure 20 shows the relative permeability curves for waterflooding and VES flooding. Honarpour's (1982) model for carbonate formations at intermediate wettability was used to calculate the relative permeability for each set using the fluids saturation and the endpoints, as expressed below[30]

https://doi.org/10.1021/acsomega.1c04900
ACS Omega 2022, 7, 504−517

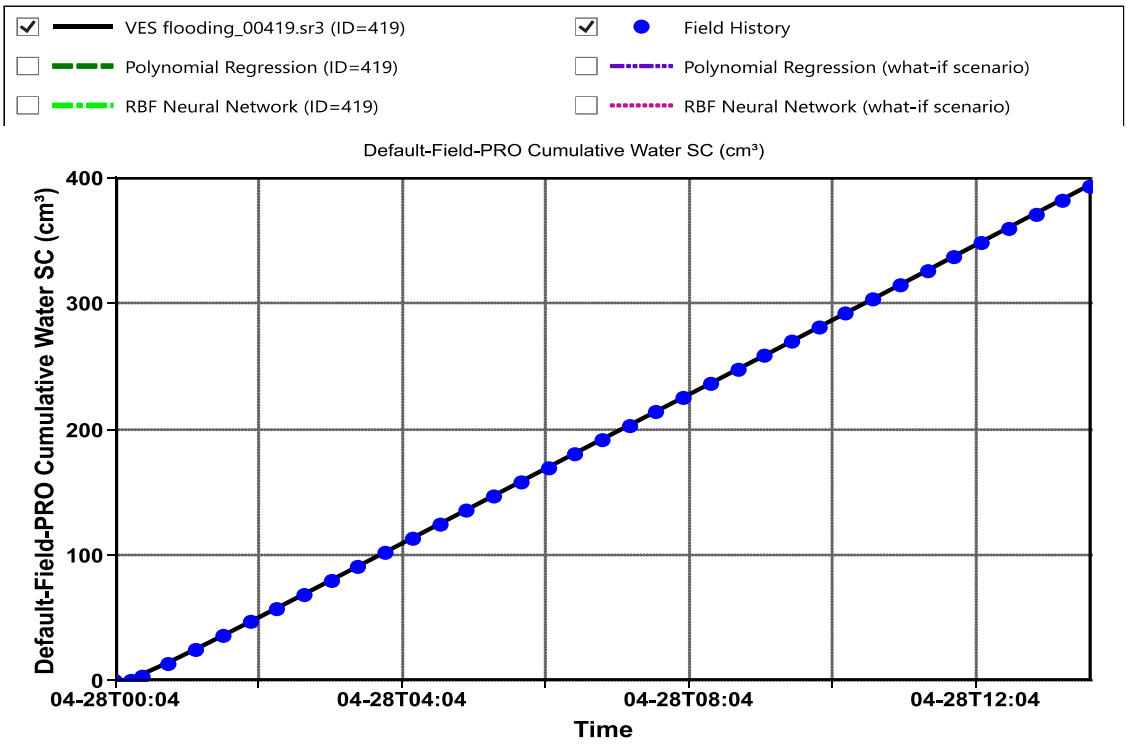

Figure 23. Optimal match for the cumulative water production obtained from the coreflooding experiment and simulation model.

$$K_{rw} = 0.29986\left(\frac{S_w - S_{wi}}{1 - S_{wi}}\right) - 0.34797\left(\frac{S_w - S_{or}}{1 - S_{wi} - S_{or}}\right)^2 (S_w - S_{wi}) + 0.413259\left(\frac{S_w - S_{wi}}{1 - S_{wi} - S_{or}}\right)^4 \quad (2)$$

$$K_{ro} = 1.2624\left(\frac{S_o - S_{or}}{1 - S_{or}}\right)\left(\frac{S_o - S_{or}}{1 - S_{wi} - S_{or}}\right)^2 \quad (3)$$

4.2.3. History Matching. Before developing the field-scale model, the simulation model was calibrated using the flooding experiments and the lab-scale results. History matching was applied to improve the reliability of the simulation model. CMG-CMOST software developed by computer modeling group (CMG) was used to perform the history matching. The target was to match the real coreflooding experiment with the simulation model outputs, at the core scale. Table 2 lists the parameters used during the history matching. Around 500 random cases were generated by varying the model parameters till achieving the best match between the measured data and the simulation output, as shown in Figure 21. The cumulative oil recovery and cumulative water production were matched with the experimental results. A very good match was obtained as shown in Figures 22 and 23; the estimation errors are 3.8% for the cumulative oil and 0.213% for the cumulative water productions.

4.2.4. Field-Scale Simulation. A giant field model was built to test the efficiency of VES flooding for enhancing the oil recovery from NFR. The studied reservoir has an average area of 336 000 acres and average porosity of 17%. The initial reservoir pressure is 2200 psi and the oil−water contact (OWC) is 4900 ft. The oil-bearing formation is bound from the top and bottom by dense argillaceous limestone with 30 to 45 ft thickness. The total pore volume is 119 MMM bbl, with an average initial oil saturation of 73.6%, above the oil−water contact. The reservoir is considered as a naturally fractured reservoir with an original oil in place (OOIP) of 39.7 MMM bbl. In general, the reservoir has a low rock permeability, between 1 and 14 mD. Recent core data

Table 2. Studied Parameters for History Matching

interpolation set	parameter	upper limit	lower limit	matched value
waterflooding	Dtrapn1	−2.358	−3.93	−3.62
VES flooding	Dtrapn2	−1.947	−3.245	−1.95
waterflooding	Dtrapw1	−2.96625	−4.94375	−4.74
VES flooding	Dtrapw2	−1.81055	−3.01758	−2.99
waterflooding	Ocrv1	1.44375	0.86625	1.26
VES flooding	Ocrv2	1.44375	0.86625	0.94
waterflooding	Wcrv1	2.26375	1.35825	2.21
VES flooding	Wcrv2	0.936625	0.561975	0.92

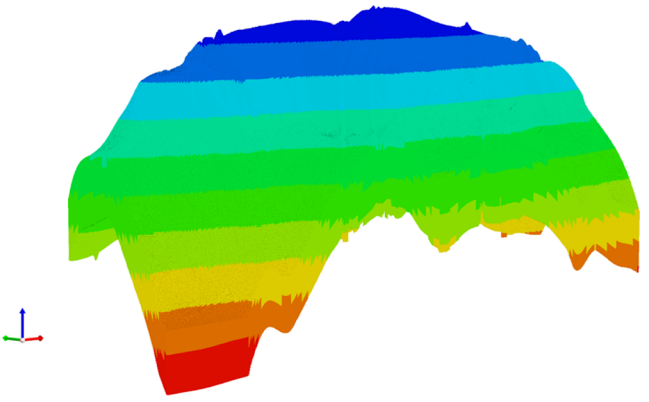

Figure 24. Three-dimensional (3D) model for the reservoir used in this work. The reservoir has 8 layers, and 1.32 million grid blocks were used in the simulation model.

https://doi.org/10.1021/acsomega.1c04900
ACS Omega 2022, 7, 504−517

proved that the horizontal and vertical permeabilities are very similar. The detailed static model properties were used in the simulation model as follows: 1.32 million grid blocks were used and the reservoir dimensions are 250 × 882 × 8, as shown in Figure 24. The production was started utilizing the natural reservoir energy, and 141 wells with a minimum bottom hole pressure of 1882 psi were used. Then, around 28 injectors were introduced in the periphery of the reservoir to inject either water or chemicals. Using the developed model, three different scenarios were examined: natural production, waterflooding, and VES injection, as will be described in full detail in the coming sections of this paper.

AUTHOR INFORMATION

Corresponding Authors

Abdullah S. Sultan − *Petroleum Engineering Department, College of Petroleum Engineering & Geosciences, King Fahd University of Petroleum & Minerals, Dhahran 31261, Saudi Arabia*; Phone: +966 (013) 860-2586; Email: sultanas@kfupm.edu.sa; Fax: +966 (013) 860-4447

Mohamed Mahmoud − *Petroleum Engineering Department, College of Petroleum Engineering & Geosciences, King Fahd University of Petroleum & Minerals, Dhahran 31261, Saudi Arabia*; Phone: +966 (013) 860-2524; Email: mmahmoud@kfupm.edu.sa; Fax: +966 (013) 860-4447

Authors

M. Elmuzafar Ahmed − *Petroleum Engineering Department, College of Petroleum Engineering & Geosciences, King Fahd University of Petroleum & Minerals, Dhahran 31261, Saudi Arabia*

Amjed M. Hassan − *Petroleum Engineering Department, College of Petroleum Engineering & Geosciences, King Fahd University of Petroleum & Minerals, Dhahran 31261, Saudi Arabia*

Complete contact information is available at: https://pubs.acs.org/10.1021/acsomega.1c04900

Notes

The authors declare no competing financial interest.

ACKNOWLEDGMENTS

The authors would like to acknowledge the College of Petroleum Engineering and Geosciences, King Fahd University of Petroleum and Minerals, Saudi Arabia, for providing the necessary laboratory facilities and KACST for providing financial support under NSTIP Project 14-OIL611-04.

REFERENCES

(1) Lake, L. W.; Johns, R.; Rossen, B.; Pope, G. A. *Fundamentals of Enhanced Oil Recovery*; Society of Petroleum Engineers: Richardson, TX, 2014; Vol. *1*, p 1.

(2) Green, D. W.; Willhite, G. P. *Enhanced Oil Recovery*; Henry L. Doherty Memorial Fund of AIME, Society of Petroleum Engineers: Richardson, TX, 1998; Vol. *6*, pp 143−154.

(3) *Enhanced Oil Recovery, II: Processes and Operations*; Donaldson, E. C.; Chilingarian, G. V.; Yen, T. F., Eds.; Elsevier, 1989.

(4) Bahadori, A. *Fundamentals of Enhanced Oil and Gas Recovery from Conventional and Unconventional Reservoirs*; Gulf Professional Publishing, 2018.

(5) Gurgel, A.; Moura, M. C. P. A.; Dantas, T. N. C.; Neto, E. B.; Neto, A. D. A review on chemical flooding methods applied in enhanced oil recovery. *Braz. J. Pet. Gas* **2008**, *2*, 83−95.

(6) Thomas, S. In *Chemical EOR−The Past, Does It Have a Future?*, SPE Distinguished Lecturer Series. SPE-108828-DL, 2006; pp 2005−2006.

(7) Cheraghian, G. In *Improved Heavy Oil Recovery by Nanofluid Surfactant Flooding—An Experimental Study*, 78th EAGE Conference and Exhibition; European Association of Geoscientists & Engineers, 2016; pp 1−5.

(8) Esfandiarian, A.; Azdarpour, A.; Santos, R. M.; Mohammadian, E.; Hamidi, H.; Sedaghat, M.; Dehkordi, P. B. Mechanistic Investigation of LSW/Surfactant/Alkali Synergism for Enhanced Oil Recovery: Fluid−Fluid Interactions. *ACS Omega* **2020**, *5*, 30059−30072.

(9) Kokal, S.; Al-Kaabi, A. In *Enhanced Oil Recovery: Challenges & Opportunities*, World Petroleum Council: Official Publication, 2010; pp 64−69.

(10) Lakatos, I. J.; Toth, J.; Bodi, T.; Lakatos-Szabo, J.; Berger, P. D.; Lee, C. H. In *Application of Viscoelastic Surfactants as Mobility-Control Agents in Low-Tension Surfactant Floods*, International Symposium on Oilfield Chemistry; OnePetro, 2007.

(11) Morvan, M.; Degre, G.; Leng, J.; Masselon, C.; Bouillot, J.; Zaitoun, A.; Moreau, P. In *New Viscoelastic Fluid for Chemical EOR*, IOR 2009-15th European Symposium on Improved Oil Recovery; European Association of Geoscientists & Engineers, 2009; p cp-124.

(12) Chierici, G. L. The Simulation of Reservoir Behaviour Using Numerical Modelling. In *Principles of Petroleum Reservoir Engineering*; Springer: Berlin, Heidelberg, 1995; pp 123−229.

(13) Boyer, C. M.; Glenn, S. A.; Claypool, B. R.; Weida, S. D.; Adams, J. D.; Huck, D. R.; Stidham, J. E. In *Application of Viscoelastic Fracturing Fluids in Appalachian Basin Reservoirs*, SPE Eastern Regional Meeting; OnePetro, 2005.

(14) Azad, M. S.; Sultan, A. S.; Nuaim, S. A.; Mahmoud, M. A.; Hussein, I. A. In *Could VES be a part of a Hybrid Option to Recover Heavy oil in Complex Heavy oil Reservoirs*, SPE Heavy Oil Conference-Canada; OnePetro, 2014.

(15) Li, K. X.; Jing, X. Q.; He, S.; Ren, H.; Wei, B. Laboratory study displacement efficiency of viscoelastic surfactant solution in enhanced oil recovery. *Energy Fuels* **2016**, *30*, 4467−4474.

(16) Sultan, A. S.; Azad, M. S.; Hussein, I. A.; Mahmoud, M. A. In *Rheological Assessment of VES as an EOR Fluid in Carbonate Reservoir*, SPE EOR Conference at Oil and Gas West Asia; OnePetro, 2014.

(17) Janjua, A. N.; Sultan, A. S.; Kamal, M. S. In *Investigation of Heavy Oil Recovery Using Sequential Viscoelastic Surfactant and Chelating Agent Solutions as EOR Fluid for HTHS Conditions Carbonate Reservoirs*, SPE Kingdom of Saudi Arabia Annual Technical Symposium and Exhibition; OnePetro, 2018.

(18) Janjua, A. N.; Sultan, A. S.; Saikia, T.; Kamal, M. S.; Mahmoud, M. Experimental Investigation of Noble Viscoelastic Surfactant and Chelating Agent for Heavy Oil Enhanced Oil Recovery in High-Pressure−High-Temperature Carbonate Reservoirs. *J. Surfactants Deterg.* **2021**, *24*, 289−300.

(19) Chhabra, R. P. Non-Newtonian Fluids: An Introduction. In *Rheology of Complex Fluids*; Springer: New York, NY, 2010; pp 3−34.

(20) Wang, D.; Xia, H.; Liu, Z.; Yang, Q. In *Study of the Mechanism of Polymer Solution with Visco-Elastic Behavior Increasing Microscopic Oil Displacement Efficiency and the Forming of Steady Oil Thread Flow Channels*, SPE Asia Pacific Oil and Gas Conference and Exhibition; OnePetro, 2001.

(21) Wang, D.; Wang, G.; Wu, W.; Xia, H.; Yin, H. In *The Influence of Viscoelasticity on Displacement Efficiency—From Micro to Macro Scale*, SPE Annual Technical Conference and Exhibition; OnePetro, 2007.

(22) Wang, D.; Xia, H.; Yang, S.; Wang, G. In *The Influence of Visco-Elasticity on Micro Forces and Displacement Efficiency in Pores, Cores and in the Field*, SPE EOR Conference at Oil & Gas West Asia; OnePetro, 2010.

(23) Degré, G.; Morvan, M.; Bouillot, J.; Zaitoun, A.; Al-Maamari, R. S.; Al-Hashmi, A. R.; Al-Sharji, H. H. In *Viscosifying Surfactants for Chemical EOR*, IOR 2011-16th European Symposium on Improved Oil Recovery; European Association of Geoscientists & Engineers, 2011; p cp-230.

https://doi.org/10.1021/acsomega.1c04900
ACS Omega 2022, 7, 504−517

(24) Chang, F. F.; Acock, A. M.; Geoghagan, A.; Huckabee, P. T. In *Experience in Acid Diversion in High Permeability Deep Water Formations Using Visco-Elastic-Surfactant*, SPE Annual Technical Conference and Exhibition; OnePetro, 2001.
(25) Sullivan, P. F.; Gadiyar, B. R.; Morales, R. H.; Holicek, R. A.; Sorrells, D. C.; Lee, J.; Fischer, D. D. In *Optimization of a Visco-Elastic Surfactant (VES) Fracturing Fluid for Application in High-Permeability Formations*, SPE International Symposium and Exhibition on Formation Damage Control; OnePetro, 2006.
(26) Elgibaly, A.; Farhat, M.; Nasr El Din, H.; A Fattah Ahmed, W. Visco-Elastic Surfactant Improves Sweep Efficiency and Interfacial Tension in Chemical Flooding. *J Pet. Min. Eng.* **2016**, *18*, 67−71.
(27) Carlisle, C.; Al-Maraghi, E.; Al-Saad, B.; Britton, C.; Fortenberry, R.; Pope, G. In *One-Spot Pilot Results in the Sabriyah-Mauddud Carbonate Formation in Kuwait Using a Novel Surfactant Formulation*, SPE Improved Oil Recovery Symposium; OnePetro, 2014.
(28) Ehrenberg, S. N.; Nadeau, P. H. Sandstone vs. carbonate petroleum reservoirs: A global perspective on porosity-depth and porosity-permeability relationships. *AAPG Bull.* **2005**, *89*, 435−445.
(29) Ahmed, M. E.; Sultan, A. S.; AlSofi, A.; Al-Hashim, H. S.; Hussaini, S. R. In *Pore-Scale Imaging to Investigate Wettability and Recovery Mechanism for Surfactant/Polymer Flooding*, SPE Russian Petroleum Technology Conference; OnePetro, 2018.
(30) Honarpour, M.; Koederitz, L.; Harvey, A. H. *Relative Permeability of Petroleum Reservoirs*; CRC Press, 2018.

https://doi.org/10.1021/acsomega.1c04900
ACS Omega 2022, 7, 504−517